

Spectral-Spatial Classification of Remote Sensing Images using a Region-based GeneSIS Segmentation Algorithm

Stelios K. Mylonas¹, Dimitris G. Stavrakoudis¹, John B. Theocharis¹, and Paris A. Mastorocostas²

Abstract—This paper proposes a spectral-spatial classification scheme for the classification of remotely sensed images, based on a new version of the recently proposed Genetic Sequential Image Segmentation (GeneSIS). GeneSIS segments the image in an iterative manner, whereby at each iteration a single object is extracted via a genetic algorithm-based object extraction method. In the previous version of GeneSIS, the candidate objects to be extracted were evaluated through the fuzzy content of their included pixels. In the present proposal, a watershed-driven fine segmentation map is initially obtained which serves as the basis for the upcoming GeneSIS segmentation. Our objective is to enhance the flexibility of the algorithm in extracting more flexible object shapes and reduce the execution time of the segmentation, while at the same time preserving all the inherent attributes of the GeneSIS procedure. Accordingly, the previously proposed fitness components are redefined in order to accommodate with the new structural components. In this work, the set of fuzzy membership maps required by GeneSIS are obtained via an unsupervised fuzzy clustering. The final classification result is obtained by combining the results from the unsupervised segmentation and the pixel-wise SVM classifier via majority voting. The validity of the proposed method is demonstrated on the land cover classification of a high-resolution hyperspectral image.

Image Segmentation; Watershed transform; Genetic Algorithms; spectral-spatial Classification; Hyperspectral Images.

I. INTRODUCTION

The rich amount of information currently available from satellite images with high spectral-spatial resolution (HSSR) poses new challenges in the field of land cover classification from remotely sensed imagery. An attractive method, recently receiving considerable attention, is to incorporate spatial information to improve the classification results obtained by traditional pixel-based classifiers. One way to achieve this goal is to extract contextual information from fixed-window neighborhoods around pixels and incorporate it to their feature vector of spectral values. The drawback of this method is that it raises the issue of scale selection, due to the existence of structures of different sizes

within the image. A more effective alternative for integrating spatial information is to perform image segmentation. Segmentation is the partitioning of the image into disjoint regions so that each region is connected and homogeneous with respect to some homogeneity criterion of interest.

Most of the existing image segmentation techniques can be distinguished into one of the following three categories [1]: clustering/feature thresholding, region growing and edge detection. Clustering techniques operate in the spectral space, searching for significant modes in the feature space. The created clusters are then mapped back to the spatial domain to form the segmentation map. Important issues to be addressed with cluster methods are the determination of the proper number of clusters and the consideration of the spatial association of pixels which is usually ignored. Region growing methods start usually from a pixel level and, using a homogeneity criterion, merge neighboring objects sequentially until the criterion exceeds a user-defined threshold. The main demerit of these methods lies on the proper selection of this threshold, which in most cases lacks physical meaning.

Edge-based methods search for discontinuities in the image by examining the existence of local edges. The extracted edges finally enclose the created objects. The watershed transformation is the most commonly used method of this category and has been employed in various remote sensing applications [2]-[4]. A significant limitation of watershed is its sensitivity to local variations, which typically results in severe over-segmentation of the image. For this reason, watershed is often incorporated into more sophisticated methods as a preliminary segmentation step. For instance, in [5] the initially created watershed objects are subsequently merged through graph partitioning techniques. Other methods try to overcome the oversegmentation problem either by using markers [3] or by applying other more advanced methods [4].

In this work, a fine segmentation map is initially obtained from watershed transformation that serves as the basis for the Genetic Sequential Image Segmentation (GeneSIS) [6], [7]. GeneSIS is an iterative segmentation algorithm, which has been applied to the object-based classification of remotely sensed images. The global segmentation problem is decomposed into a succession of simpler tasks, i.e. the extraction of a unique object at each iteration. GeneSIS exploits the searching capabilities of genetic algorithms (GAs) with the aim to locate spatially the proper objects to be extracted from the image. The watershed objects are regarded now as structural units, instead of pixels, and the generated segments from GeneSIS are a collection of connected

¹ Department of Electrical and Computer Engineering, Aristotle University of Thessaloniki, ² Department of Computer Engineering, Technological Education Institute of Central Macedonia, Serres, Greece. {smylonas@auth.gr; jstavrak@auth.gr; theochar@eng.auth.gr; mast@teicm.gr }

This research has been co-financed by the European Union (European Social Fund – ESF) and Greek national funds through the Operational Program "Education and Lifelong Learning" of the National Strategic Reference Framework (NSRF) - Research Funding Program: ARCHIMEDES III. Investing in knowledge society through the European Social Fund.

watersheds. The required labeling of the watershed objects is accomplished here by applying the fuzzy integral approach. A significant modification to the previous version of GeneSIS is that a watershed is regarded as internal of a candidate object, if its geographic centroid is included in the basic search frame of rectangular shape. Also, the marking selection scheme and the fitness function components are now reformulated so as to accord with the region-based representation.

The proposed framework offers a number of assets as described in the following. First, compared to the pixel-based treatment, the region-based representation eliminates the noise corrupting single pixels. Further, it increases the observation scale thus providing a better estimation of the local properties of the data. Secondly, the consideration of watershed regions as the new structural elements along with their own boundaries, allows GeneSIS to extract more flexible shapes. Third, the region-based GeneSIS is more robust in terms of average performance, while on the other hand it achieves similar best accuracies. Finally, owing to the initial watershed map, the suggested scheme has considerably lower computational demands compared to the pixel-based GeneSIS.

The rest of the paper is organized as follows. In Section II, we provide a general description of the proposed scheme, whereas Section III focuses on the GA part of GeneSIS, the object extraction algorithm (OEA). Experimental results on the classification of a hyperspectral image are presented in Section IV, and the paper concludes in Section V with some final remarks.

II. GENERAL CONFIGURATION

The architecture of the proposed scheme is depicted in Fig. 1. Initially, the watershed algorithm is applied in order to create a preliminary segmentation map. Unsupervised clustering by fuzzy c-means (FCM) is used here to create the fuzzy membership maps (FMMs), where each pixel is assigned a fuzzy value to its cluster label. Any other fuzzy clustering method could be used equivalently. The fuzzy degrees of pixels contained in each watershed object are combined via the fuzzy integral fusion method to compute the fuzzy values of the watershed to the different clusters, as well as assign to it a specific cluster label. The cluster-labeled connected components of watershed objects along with their membership values operate as input to the GeneSIS segmentation approach. The segmentation result produced by GeneSIS is then combined via majority voting with the fuzzy output SVM (FO-SVM) to create the final classification map.

A. Watershed Segmentation

Watershed transform is a morphological approach widely used in image segmentation. The image, considered as a topographic surface, is flooded from its minima and dams are built in order to prevent merging of water from different sources. Dams represent the watershed lines, enclosing the catchment basins. Watershed transform is usually applied to a gradient image, so that catchment basins correspond to

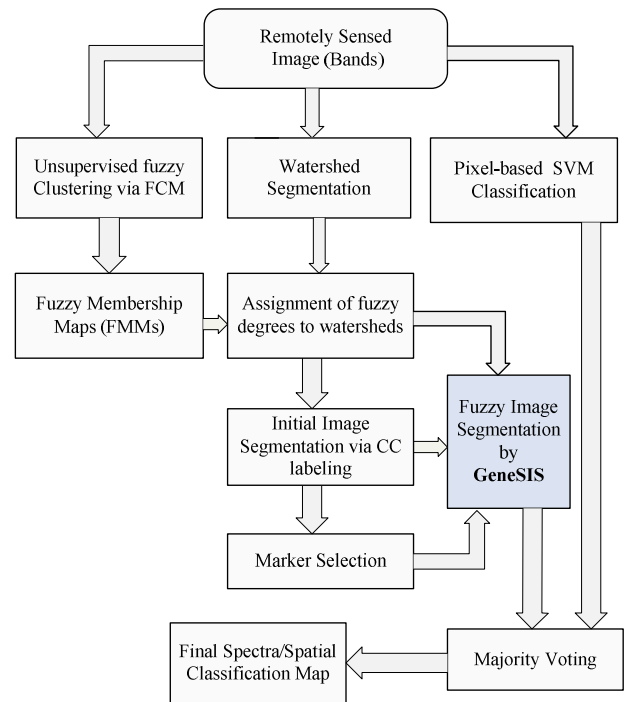


Fig. 1. Flowchart of the proposed scheme.

homogeneous regions. Among the different approaches investigated in [2] to obtain gradient images from hyperspectral data, we use the Robust Color Morphological Gradient (RCMG) method [8]. To reduce the oversegmentation resulting from watershed, two techniques were applied. First, before proceeding to the gradient estimation, a 3x3 median filter is applied on the image bands in order to smooth the surface, but at the same time preserve the significant edges. Secondly, the gradient thresholding method [9] is used, where pixel gradients with value lower than a given threshold are set to zero. With this step, small heterogeneity effects are removed while neighboring watersheds with low gradient values are merged.

The watershed implementation presented in [10] has been used in this work. As a result of the segmentation, a set $\mathcal{W} = \{W_i / i = 1, \dots, \Omega(\mathcal{W})\}$ of watershed objects is obtained, along with the set of watershed pixels representing the edges between regions ($\Omega(\cdot)$ denotes the crisp cardinality operator). The assignment of the watershed pixels to the neighboring objects is carried out as described in [2]. For each W_i , the standard vector median is computed:

$$x_{VM}^i = \arg \min \left\{ \sum_{x_j \in W_i} \|x - x_j\|_1 \right\}, \quad (1)$$

and every watershed pixel is assigned to its neighboring object with the “closest median”, i.e. the distance between the vector median of this region and the watershed pixel vector is minimal.

B. Fuzzy Membership Maps via Clustering

Clustering is used to partition a data set into a number of

clusters, so that members of the same cluster are spectrally similar to each other. Contrary to hard clustering, fuzzy clustering methods provide for each pattern a degree of belongingness to every cluster. Specifically, after clustering each pixel $x \in \mathcal{I}$ receives a vector with the associated fuzzy membership degrees:

$$\mu(x) = [\mu_1(x), \dots, \mu_j(x), \dots, \mu_c(x)], \quad (2)$$

where c is the number of clusters. Based on these values, each pixel is assigned to a cluster label, following the max argument principle:

$$\mathcal{L}(x) = \arg \max_{j=1, \dots, c} \{\mu_j(x)\}, \quad (3)$$

where $\mathcal{L}(\cdot)$ is the cluster label assignment function and $\mathcal{L}(x) \in \{L_1, \dots, L_j, \dots, L_c\}$. As a result of clustering, c fuzzy membership maps (FMMs) are created. These maps contain all the important information required at the following stages of our method. Any unsupervised fuzzy clustering method can be used. In this work, we employed the standard fuzzy c-means (FCM) algorithm, a popular technique of this category.

C. Assignment of Fuzzy Degrees to Watershed Objects

In the proposed classification scheme, we regard watershed objects as structural units, instead of pixels. So, before proceeding to the image segmentation by GeneSIS, we need to determine the fuzzy content of each watershed object at the various cluster labels. To accomplish this task, the decision fusion approach of fuzzy integral is employed, which is defined with respect to a fuzzy measure, usually a g_λ -fuzzy measure. Fuzzy integral has been used in previous works to combine the results of multiple classifiers [11].

Here, all pixels contained in a watershed object are regarded as different (equivalent) sources of fuzzy information. Then, the fuzzy degrees conveyed by pixels will be combined via decision aggregation to produce the membership values of watershed objects.

Let us consider an arbitrary watershed object $W_i = \{x_j^i / j=1, \dots, \Omega(W_i)\}$, where each pixel x_j^i retains a vector $\mu(x_j^i)$ of fuzzy degrees. To calculate the membership degree of W_i to label $k \in \{1, \dots, c\}$, we proceed along the following steps:

- 1) The fuzzy densities g_k^j represent the degree of importance of $\mu_k(x_j^i)$ toward the final evaluation. In our case, these densities are determined locally by considering a 3x3 neighborhood $N(x_j^i)$ of each pixel. Specifically, g_k^j is defined as the fuzzy coverage of label k in $N(x_j^i)$ of the examined pixel:

$$g_k^j = \sum_{\substack{x \in N(x_j^i) \\ \mathcal{L}(x) = L_k}} \mu_k(x) \quad (4)$$

These densities are then normalized so as $\sum_{j=1}^{\Omega(W_i)} \sum_{k=1}^c g_k^j = 1$.

- 2) Calculate the unique root $\lambda > -1$ of the equation

$$\lambda + 1 = \prod_{j=1}^{\Omega(W_i)} (1 + \lambda g_k^j). \quad (5)$$

- 3) Sort the elements of $\{\mu_k(x_j^i)\}$ in descending order: $\mu_k(x_{j_1}^i), \dots, \mu_k(x_{j_{\Omega(W_i)}}^i)$ with $\mu_k(x_{j_1}^i)$ denoting the highest membership value.

- 4) Sort the densities correspondingly, i.e. $g_k^{j_1}, \dots, g_k^{j_{\Omega(W_i)}}$.

- 5) Set $g(1) = g_k^{j_1}$ and calculate the rest fuzzy measures according to the following recursion:

$$g(l) = g_k^{j_l} + g(l-1) + \lambda g_k^{j_l} g(l-1), \quad 2 \leq l \leq \Omega(W_i). \quad (6)$$

- 6) Finally, the membership value of W_i to label k is computed as:

$$\mu_k(W_i) = \max_{l=1}^{\Omega(W_i)} \left\{ \min \left\{ \mu_k(x_{j_l}^i), g(l) \right\} \right\}. \quad (7)$$

D. Connected Component Labeling

Based on the above values, each watershed object is assigned to a cluster label, its dominant label, following the max argument principle:

$$\mathcal{L}(W) = \arg \max_{j=1, \dots, c} \{\mu_j(W)\}. \quad (8)$$

Adjacent watershed objects of the same cluster label can now be connected and are considered as hyper objects. This is achieved by applying a connected-component (CC) labeling algorithm, which merges spatially connected watershed objects that belong to the same cluster into a single hyper object. As a result, we obtain a cluster-based segmentation map containing the set of CCs: $\mathcal{C} = \{C_j / j=1, \dots, \Omega(\mathcal{C})\}$. Further, each CC shares the same cluster label with its watershed objects: $\mathcal{L}(C_j) \in \{L_1, \dots, L_j, \dots, L_c\}$. The set of CCs is used in GeneSIS segmentation to accommodate the following tasks: estimate the size of components appearing in the uncovered area of the image, and delineate the active areas of the population chromosomes to be extracted as objects.

E. Marker Selection

After the formation of cluster-based CCs, we proceed to the marker selection step. Contrary to [7], marking is now performed on watershed objects instead of pixels. The watersheds to be marked are selected according to their size and their attributed fuzzy degrees. As a first step, we choose the watersheds with area larger than a specified threshold Ω_{\min}^C , which represents approximately, the area of the smallest region of interest we want to recognize.

Next, for the previously selected watersheds we consider the difference $\Delta\mu(W) = \mu_{dom}(W) - \mu_{comp}(W)$, where $\mu_{dom}(W)$ is the highest fuzzy degree in the dominant cluster label and $\mu_{comp}(W)$ denotes the second highest degree associated with the most competing label. Since the membership values given by FCM are tight to unity, $\Delta\mu$ is an indication of the confidence of the examined watershed. Large watersheds with degree difference above a defined fuzziness threshold

$\Delta\mu(W) > \Delta\mu_{th}$ are selected as markers. The value of $\Delta\mu_{th}$ depends on the uncertainty from the clustering result. Highly mixed images need lower values, while those partitioned confidently take a higher one. Concluding, the most reliable watersheds will be marked with the goal to retain their label after segmentation by GeneSIS, and hence, prevent under-segmentation. Spatial regions not including markers are regarded as ambiguous and their label might change after GeneSIS. In the sequel, a cluster-based CC containing a marked watershed will be denoted as $C_i^{(m)}$.

F. Segmentation by GeneSIS

In this stage the GeneSIS algorithm is performed, adapted to operate on a region-based image representation obtained by watershed transform. Each object extracted by GeneSIS is now considered as an aggregation of connected watershed objects existing in the terrain. Our aim with this step is to reduce the oversegmentation of watershed partition as well as the one of the cluster-based segmentation maps. Specifically, the objective is to partition the image into larger, more homogeneous and well shaped regions. An outline of the proposed segmentation algorithm is shown in Fig. 2. In the following, we describe the different parts of GeneSIS.

1) *Iterative Object Extraction*: GeneSIS is a sequential procedure, where at each iteration t , a unique object S_t is extracted. Due to the iterative nature of GeneSIS, the covered part of the image gradually increases after each iteration. Henceforth, the set of extracted segments up to iteration t will be denoted as $\mathcal{S}(t)$, with the initial condition $\mathcal{S}(0) = \emptyset$. On the other hand, the uncovered part of the image is constantly decreasing. So we need to define the set of uncovered cluster-based CCs after iteration t , which is denoted as $RC(t)$ and is initialized to the initial CCs, $RC(0) = \mathcal{C}$.

2) *Size estimation of uncovered area*: Given $RC(t-1)$ and prior to the object search at iteration t , we compute the mean $A_{avg}(t)$ and standard deviation $A_{std}(t)$ of the area of all spatial structures existing in the uncovered part of the image. These quantities give an approximate view of the distribution of the remaining structures' area, thus providing an estimation of the spatial scale to be searched in the sequel. They will be used by the Object Extraction Algorithm (OEA), in order to adjust the region growing capabilities of the GA individuals and adapt the object search to the spatial characteristics of the currently uncovered area. In their calculation, we exclude insignificant CCs with area smaller than Ω_{min}^c . Finally, $A_{avg}(t)$ and $A_{std}(t)$ are updated after a fixed number of iterations (e.g. 20), in order to reduce computational demands.

3) *Object extraction algorithm*: The object extraction algorithm (OEA) is the fundamental part at each extraction iteration, being implemented by a genetic algorithm (GA). Each individual in the population represents a different object and the evolutionary process tries to find the best possible object, by minimizing a specially designed fitness function. At the end of the GA, the elite individual contains the extracted object S_t which is extracted with its own cluster label. A

GeneSIS Algorithm

- 1: **Input**: The membership values of watersheds
The cluster-based CCs
The set of markers of different labels
- 2: Initialize the sets of segmented and uncovered regions:
 $\mathcal{S}(0) = \emptyset$, $RC(0) = \mathcal{C}$
- 3: Set $t = 1$
- 4: **Repeat**
- 5: Estimate the size of the remaining objects
 $\{A_{avg}(t), A_{std}(t)\}$
- 6: Search for a new object S_t via OEA:
 $S_t \leftarrow OEA(RC(t-1), A_{avg}(t), A_{std}(t))$
- 7: Adjust the covered / uncovered areas $\mathcal{S}(t), RC(t)$
- 8: $t \leftarrow t + 1$
- 9: **Until** the $P\%$ of the image has been covered
- 10: Merge small remaining components via region growing
- 11: **Output**: The final segmentation map of the image

Fig. 2. Outline of GeneSIS procedure.

detailed description of OEA is provided in section III.

4) *Adaptation of covered and uncovered areas*: After the extraction of S_t , the set of extracted segments is updated as:

$$\mathcal{S}(t) = \mathcal{S}(t-1) \cup S_t. \quad (9)$$

At the same time, we need to update the remaining part of the image. So, the watershed components of S_t are removed from the set $RC(t-1)$ and each $C_j \in RC(t-1)$ is rearranged as follows:

$$C_j \leftarrow C_j \setminus (C_j \cap S_t), \quad (10)$$

where $A \setminus B = \{x | x \in A, x \notin B\}$, in order to create the $RC(t)$. The iterative process terminates, when a specified percentage P of the whole image has been covered (e.g. $P = 90\%$).

5) *Assignment of remaining parts*: The remaining part is mainly composed of small regions of uncertain label, dispersed around the image. These regions are finally apportioned to the already extracted objects via M-HSEG [12], a marker-based region growing method. The already extracted objects are considered as markers, with label the one assigned to them after GeneSIS. Also, the marker set contains the initially marked watersheds that have not been extracted yet. During the iterative region growing, merges between markers of different labels are prevented. The merging process stops when all unmarked watersheds are absorbed. The decision upon which pair of objects should be merged each time is made using a dissimilarity criterion. Since our algorithm operates on the fuzzy space of membership values instead of the spectral space, we employ the fuzzy region dissimilarity measure proposed in [5].

G. Spectral-Spatial Classification

Support vector machines (SVM) is a valuable classifier from machine learning that has attracted recently considerable

interest in the analysis of remote sensing images. Further, it is well recognized that the availability of fuzzy degrees of pixels to the various classes provides a better description of the image context. To this end, we perform a pixel-based classification using the fuzzy output SVM approach [13]. Following the one-versus-all (OVA) decomposition strategy, we first construct an ensemble of M binary SVMs $\{f_1(x), \dots, f_j(x), \dots, f_M(x)\}$, where M is the number of classes and $f_j(x)$ denotes the decision function of the j th classifier, trained independently to discriminate class j from the rest of the classes. Then, the method manipulates the SVM decision values, providing for each pixel a membership vector:

$$D(x) = [d_1(x), \dots, d_j(x), \dots, d_M(x)]. \quad (11)$$

After GeneSIS segmentation, the image is partitioned into a set of objects. Following the spectral-spatial rationale [6], objects are finally assigned to the various class labels by combining the segmentation map with the pixel-based SVM classification results, via majority voting. Thus, all watershed regions lying within this object are assigned to the most frequent class label.

III. OBJECT EXTRACTION ALGORITHM

As mentioned earlier, OEA is a GA-based routine, each time searching for the best possible object to be extracted from the uncovered area of the image. Over the next subsections, we describe the main issues of the GA, such as the individual's encoding, the population initialization, the fitness function and the genetic operators used.

A. Chromosome Encoding

Each individual represents a candidate object for extraction and is associated with a so-called basic search frame (BSF). BSFs are represented here as rotated rectangles of varying size and orientation. An individual of the population is encoded as a sequence of five real-coded genes:

$$O_k = (x_1^{(k)}, y_1^{(k)}, x_2^{(k)}, y_2^{(k)}, \mathcal{G}^{(k)}), \quad (12)$$

where $(x_1^{(k)}, y_1^{(k)})$ and $(x_2^{(k)}, y_2^{(k)})$ represent the upper-left and lower-right corners of an axis-aligned rectangle and $\mathcal{G}^{(k)} \in [-90^\circ, 90^\circ]$ is the rectangle's orientation with respect to the vertical axis.

In this version of GeneSIS, where watershed objects are regarded as structural units, it is not straightforward to define which objects should be contained in BSF. We choose to consider as internal, those objects whose geometric centroid is included within the borders delineated by BSF. In that respect, a BSF can be viewed as spatial loop placed somewhere over the image, which embraces a collection of adjacent watershed regions.

B. Population Initialization

Exploiting the information contained in $RC(t-1)$, the individuals of the initial population are placed at spatial regions covered by large CCs. Particularly, in order to

create O_k , we select randomly a component $C_k \in RC(t-1)$ with a probability proportional to its area, and find its bounding box of arbitrary orientation $BB(C_k)$, where $BB(\cdot)$ denotes the bounding box operator. The bounds of $BB(C_k)$ are next expanded along all its directions by a random offset $\delta \in [1, \tau]$, where τ is relatively small integer (e.g. $\tau = 20$), so as to create the O_k . The above initialization assures that the evolutionary search will be focused mostly on large and uncovered areas.

C. Active Region Determination

When evaluating candidate solutions, we are particularly interested in obtaining an object the major part of which is homogeneous, i.e., it contains watersheds with high fuzzy degrees in the same cluster label. Nevertheless, owing to the genetic evolution, an object may be located spatially in such a way that some watersheds included in the BSF are already extracted at previous invocations of the OEA, while some others are marked with a different label. To cope with this situation, an object O_k is evaluated in terms of the so called active area, denoted as $AR(O_k)$.

The determination of the active area is accomplished as follows. In the first step, we remove from O_k watersheds extracted from previous calls of OEA, since our main objective is to segment currently uncovered regions of the image. Let us define the overlapping region between O_k and the already extracted segments S_i :

$$OVE(O_k) = O_k \cap S(t-1). \quad (13)$$

The remaining area O'_k , obtained by excluding $OVE(O_k)$ from O_k is determined by

$$O'_k = O_k \setminus OVE(O_k). \quad (14)$$

Next, we determine the dominant cluster label of the individual. This is decided on the basis of the fuzzy coverage of O'_k for the different cluster labels:

$$\tilde{\Omega}_j(O_k) = \sum_{\substack{W \in O'_k \\ \mathcal{L}(W) = L_j}} \Omega(W) \mu_j(W). \quad (15)$$

$\tilde{\Omega}_j(O_k)$ indicates the fuzzy degree to which watersheds of label j exist in O'_k . Finally, the dominant label of O_k is derived via the max argument rule:

$$\mathcal{L}(O_k) = \arg \max_{j=1, \dots, c} \{\tilde{\Omega}_j(O_k)\}. \quad (16)$$

Generally, the sub-area O'_k includes watersheds of the object's cluster label, as well as watersheds assigned to different labels. The former are regarded as positive examples (PEs) whereas the latter ones are considered as negative examples (NEs). The homogeneity property of a region dictates that O'_k should contain as many PEs as possible with strong fuzzy degrees, and a smaller portion of NEs, preferably with lower degrees to other labels. A special occasion of interest occurs when O'_k includes sections of NEs with

marked watersheds inside. Let us define these sections as a set comprising the marked overlapping regions of O'_k with the uncovered CCs of different labels:

$$OVM(O_k) = \bigcup_{\substack{j=1 \\ \mathcal{L}(C_j) \neq \mathcal{L}(O_k)}}^{\Omega(RC(t-1))} (O'_k \cap C_j)^{(m)}. \quad (17)$$

In the following, $OVM(O_k)$ is excluded from O'_k . This is explained by noticing that, based on the marker selection scheme (Section II.E), marked image parts are considered as large and confident regions, as dictated by cluster-based analysis. Thus, it seems reasonable to allow them be absorbed by a different object at a subsequent invocation of OEA. Moreover, with this removal we avoid under-segmentation, since the object is prevented from expanding into regions of possibly different label. The active area of a candidate solution is now formulated as follows:

$$AR(O_k) = O_k \setminus (OVE(O_k) \cup OVM(O_k)). \quad (18)$$

Finally, an important requirement of our method is that the active area should be a connected component. This constraint is imposed in order to avoid the extraction of spatially disjoint segments of the same label from a single call to the OEA. The connectedness condition is satisfied by applying on $AR(O_k)$ the CC labeling algorithm. In case that the active area is not connected, we find the component with the largest area $ARC_{\max}^{(k)}$, and consider this component as the new active region, i.e. $AR(O_k) = ARC_{\max}^{(k)}$.

After the previous readjustments, $AR(O_k)$ is a subset of O_k and its location may differ significantly from the corresponding rectangular area of BSF. For this reason, chromosome is repaired and limited to the bounding box of its active region, i.e.:

$$O_k^{rep} = BB(AR(O_k)). \quad (19)$$

Henceforth, we will consider that chromosomes have been repaired and that their active region is connected. The active area represents the useful region of an individual; its fuzzy content is exclusively employed in the fitness function calculations, discussed next.

D. Fitness Function

The determination of fitness function is of particular importance for the GA and hence the OEA. The suggested fitness function design aims at fulfilling three goals simultaneously: the extracted objects should be large, homogeneous (that is, they should not contain mixed regions of different labels), and smoothly shaped. The first two objectives are attained by means of the coverage and consistency criteria, while for the third one we devise a suitable smoothness criterion. All fitness components are computed in a fuzzy manner by manipulating the fuzzy degrees of watersheds to the cluster labels.

Given the dominant label of O_k , we define the fuzzy coverage of the PEs and NEs, respectively, covered by the active area of O_k :

$$\tilde{\Omega}_p(O_k) = \sum_{\substack{W \in AR(O_k) \\ \mathcal{L}(W)=L_j, \mathcal{L}(W) \neq \mathcal{L}(O_k)}} \Omega(W) \mu_j(W), \quad (20)$$

$$\tilde{\Omega}_n(O_k) = \sum_{\substack{W \in AR(O_k) \\ \mathcal{L}(W)=L_j, \mathcal{L}(W) \neq \mathcal{L}(O_k)}} \Omega(W) \mu_j(W). \quad (21)$$

The coverage criterion promotes the extraction of large objects by maximizing the fuzzy coverage of PEs. The notion of a large object is strongly related to the size of existing components in the uncovered part of the image, and therefore differs along the various extractions of GeneSIS. In order to match the GA search to the currently available components size, we define a threshold value $A_{thr}(t)$ that is considered as an estimate of a large object's area:

$$A_{thr}(t) = A_{avg}(t) + A_{std}(t). \quad (22)$$

The coverage fitness $f_{COV} \in [0,1]$ is then defined by passing $\tilde{\Omega}_p(O_k)$ through the following monotonically increasing sigmoid function:

$$f_{COV} = \frac{1}{1 + e^{-b(\tilde{\Omega}_p(O_k) - A_{avg}(t))}}. \quad (23)$$

Parameter b controls the slope of the sigmoid; it is defined so that for the threshold value $A_{thr}(t)$ we obtain a large coverage value d (for example, $d = 0.99$). Notice that objects with $\tilde{\Omega}_p(O_k) = A_{avg}(t)$ are assigned a fitness value $f_{COV} = 0.5$, thereby being regarded as solutions of moderate quality. In addition, highly qualified solutions with $f_{COV} \cong 1.0$ are obtained for objects whose active areas fulfill the condition $\tilde{\Omega}_p(O_k) \geq A_{thr}(t)$. As a result, GA search is properly adapted to the scale of the uncovered area of the image, while at the same time promotes the extraction of large objects, thus avoiding oversegmentation.

Consistency serves as a measure of the region's homogeneity, acting along an opposite direction to the coverage criterion. It prevents the continuous growing of an object and its expansion into highly mixed regions, thereby avoiding under-segmentation. Let $\tilde{G}_p(O_k)$ denote the cumulative degrees of NEs to the object's label:

$$\tilde{G}_p(O_k) = \sum_{\substack{W \in AR(O_k) \\ \mathcal{L}(O_k)=L_j, \mathcal{L}(W) \neq \mathcal{L}(O_k)}} \Omega(W) \mu_j(W). \quad (24)$$

This term represents the penetration of the dominant label in NEs and is an indication of their ambiguity. NEs with higher values of \tilde{G}_p are more consistent than those with low values of \tilde{G}_p . Finally, the consistency fitness $f_{CONS} \in [0,1]$ is defined as follows:

$$f_{CONS} = \begin{cases} 0, & \tilde{\Omega}_p + \tilde{G}_p \leq \tilde{\Omega}_n \\ \frac{(\tilde{\Omega}_p + \tilde{G}_p) - \tilde{\Omega}_n}{(\tilde{\Omega}_p + \tilde{G}_p)}, & \text{otherwise.} \end{cases} \quad (25)$$

A zero consistency value is assigned to those objects that cover more NEs than PEs. The fitness value then increases linearly to 1 when the number of NEs diminishes. Thereby,

consistency encourages the formation of objects covering a large number of confident PEs and fewer NEs.

The third fitness component quantifies the smoothness of the object and serves as a measure of textural homogeneity, since it evaluates the shape of the object. Objects with strongly irregular shape are penalized, to avoid the simultaneous extraction of spatially distant regions of the same label. Smoothness is defined as the ratio between the area of $AR(O_k)$ and the area of its arbitrary oriented bounding box:

$$f_{SMO}(O_k) = \frac{\Omega(AR(O_k))}{\Omega(BB_k)}, \quad (26)$$

where $BB_k = BB(AR(O_k))$. The above quantity measures the matching degree of an object with the rectangular prototype shape. Objects with nearly rectangular shapes receive high f_{SMO} values, while those with irregular shapes are penalized.

The overall fitness function is obtained by combining the above three criteria:

$$f = f_{COV} \cdot f_{CONS} \cdot f_{SMO}. \quad (27)$$

During the initial iterations where the image is mostly uncovered, the OEA extracts large and pure objects, which fulfill both coverage and consistency criteria to a high degree. As the image is progressively segmented, the OEA spatially achieves an optimal balance between coverage (region growing) and consistency (homogeneity), while maintaining the shape of the object into acceptable limits.

E. Genetic Operators

The well-known one-point crossover operator is applied here with a probability p_c . In the mutation, each gene is chosen with a probability p_m and assigned to a random value from its domain. The mutation rate is defined as the inverse of the number of genes in the solution encoding (0.2 here). Tournament selection is used for selecting individuals to be recombined for the next generation, while elitism ensures that the fittest solution is retained during evolution. The above operators comprise the main mechanism of the search procedure. Starting from the initial population of rectangles and through crossover and mutation operators, new rectangles are created at each generation of the GA. Thus the search space is explored and via the survival of the fittest individuals the GA leads to a desirable solution. The algorithm terminates after a maximum number of iterations, or when the fitness value of the best individual does not increase after a fixed number of generations.

At the end of each generation, a specially designed local tuning operator [7] is applied on the elite individual to improve its fitness. After the first generations, the population usually converges to a specific region, so this operator assists in finding quickly a better solution, thus boosting spatial search.

IV. EXPERIMENTAL RESULTS

The proposed methodology was tested on a hyperspectral image, acquired by the ROSIS-03 sensor over the University of Pavia, northern Italy. The image is 610×340 pixels with a

spatial resolution of 1.3 m/pixel. The number of spectral bands in the original image is 115, with a spectral range from 0.43 to 0.86 μm . The 12 noisiest channels have been removed and the remaining 103 were used in our experiments. A three-band true color composite and the reference data are shown in Fig. 3(a) and (b), respectively. For the number of training and testing samples per class, the reader can refer to [7].

Watershed segmentation is initially performed as described in section II.A and the resulting map is shown in Fig. 3(c). In this image each watershed is represented by its mean spectral value on an arbitrarily chosen band (Band 60). As expected, the image is highly oversegmented containing small, well-shaped and compact watershed regions, with the exception of some larger components resulting after gradient thresholding. This fine segmentation result forms the initial map of structural elements used as the basis for the GeneSIS operation. After the assignment of the watershed pixels to their neighboring objects, a segmentation map with 9,152 initial watersheds is created.

For the generation of FMMs, FCM clustering is performed with $c = 9$ clusters (equal to the number of classes). The FCM algorithm is applied on a reduced space of ten features obtained by applying the PCFA method [14]. The method selects ten distinguishing groups of adjacent bands: 1-4, 5-10, 11-24, 25-35, 36-43, 44-68, 69-72, 73-75, 76-79, and 80-103. The spectral values are then computed by averaging over the bands pertaining to each group. After computing the membership degrees of watershed objects via fuzzy integral, we apply the CC labeling algorithm with four neighborhood connectivity. The resulting cluster-based segmentation map is shown in Fig. 3(d), where different colors correspond to different cluster labels. This map contains 2,053 objects, considerably fewer than watershed segmentation. Nevertheless, over-segmentation is still observed, since several ground truth components of meadows and bare soil are split into different cluster labels.

In the marker selection stage, we set $\Omega_{\min}^C = 20$ as the size of structures to be marked, in order to enable GeneSIS recognize the small components of trees and shadow classes. The global threshold of fuzziness $\Delta\mu_{th}$ is set to the median of $\Delta\mu(W)$, specifically $\Delta\mu_{th} = 0.35$. As a result, 4,218 watersheds are selected for marking, less than half of the ones contained in the initial watershed segmentation map.

In the following, we proceed to image segmentation by GeneSIS. Table I shows the GA parameters of OEA used in our experiments. Due to the stochastic nature of GeneSIS, we performed 30 independent runs with random initial seeds, to obtain a robust assessment of our methodology. GeneSIS terminates when the 90% of the image has been covered. The remaining components are merged to the previously extracted objects via region growing. One of the segmentation maps obtained by GeneSIS is displayed in Fig. 3(e), where 1,315 segments were extracted. On average, GeneSIS generated 1,304.15 objects, considerably smaller than the initial number of 9,152 connected components. In addition, it should be stressed that the extracted objects appear with varying shapes

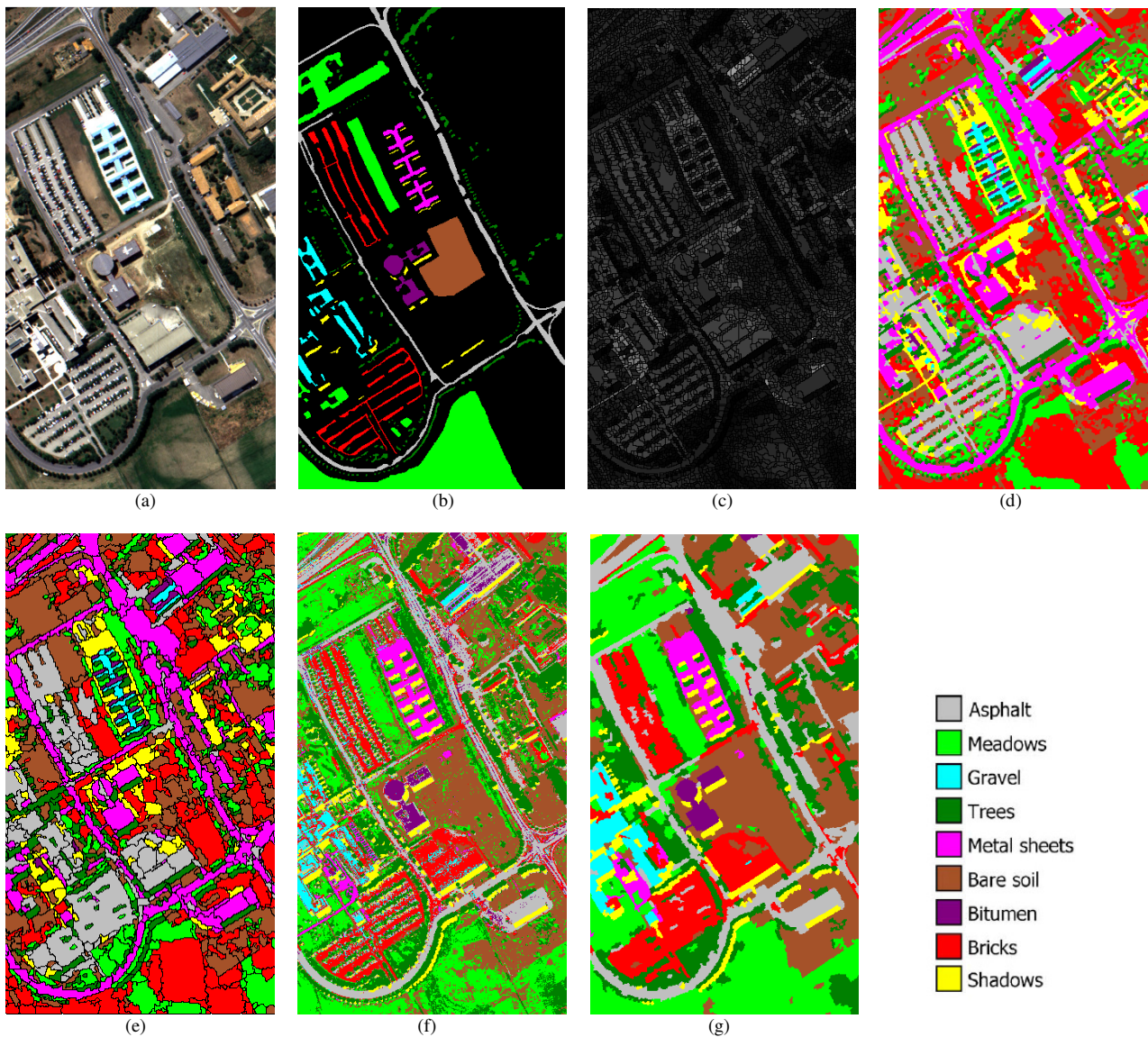


Fig. 3. *University of Pavia* image. (a) Three-band color composite. (b) Reference sites. (c) Watershed segmentation map. (d) Unsupervised cluster-based segmentation map by FCM clustering. (e) Segmentation map after GeneSIS and merging of small components. (f) SVM pixelwise classification map. (g) Final classification map.

and irregular boundaries. Particularly, their shapes are delineated from the boundaries of watershed objects included in the BSFs. This is a major difference to the previous version of GeneSIS where, depending on the parameter settings of the smoothness fitness, the delineated boundaries were affected more strongly by the rectangular shape of BSFs.

Pixel-based classification is performed by fuzzy output SVM using the complete space of 103 spectral bands. The RBF kernel was considered while the optimal parameters were chosen by 5-fold cross validation: $C = 8$ and $\gamma = 2^{-5}$. After hardening of fuzzy degrees, we obtain the supervised classification map shown in Fig. 3(f). As can be seen, most of the classes are correctly classified, with the exception of the large meadows region in the lower part of the image. Due to high spectral similarity, SVM confuses meadows, primarily

with bare soil and the trees classes. Furthermore, in the absence of contextual information, the SVM map is highly fragmented. This map is next combined with the GeneSIS segmentation result via majority voting to obtain the final classification result. The classification map corresponding to the segmentation map of Fig. 3(e) is depicted in Fig. 3(g), exhibiting an overall classification accuracy of 95.35%. The result classifies accurately the image scene and resolves the mixing of the meadows area in the lower part of the image.

Table II hosts the classification results of pixel-wise SVM, the pixel-based and region-based versions of GeneSIS, along with two other object-based approaches. *Wat+MV* stands for majority voting performed within each watershed object, individually [2]. Finally, minimum spanning forest (MSF) [15] is a region growing method, requiring a set of class-labeled markers. In order to obtain these markers, the

TABLE I. PARAMETERS USED IN THE OEA

Parameter	Value
Maximum number of generations	1000
Number of generations allowed without change	80
Population size	20
Tournament size	2
Crossover probability	0.8
Mutation probability	0.2

TABLE II. CLASSIFICATION ACCURACIES FOR THE UNIVERSITY OF PAVIA IMAGE

	SVM	Pixel-based GeneSIS	Region-based GeneSIS	Wat + MV	MSF
OA _{avg}	-	90.95	92.06	-	-
OA	81	95.27	95.35	87.08	88.55
AA	88.15	95.81	95.54	93.32	92.61
k	75.74	93.67	93.76	83.34	85.14
Asphalt	76.51	94.62	94.32	90.63	96.84
Meadows	73.59	94.96	95.66	78.25	80.46
Gravel	71.35	92.18	86.94	79.06	74.55
Trees	98.70	88.87	89.32	97.97	92.89
Metal sheets	99.01	96.05	98.74	99.46	99.91
Bare soil	91.80	98.99	98.43	97.24	98.23
Bitumen	91.54	99.18	98.37	98.78	99.59
Bricks	91.14	97.89	98.04	98.63	99.67
Shadows	99.75	99.50	100	99.87	91.32

procedure described in section II.C-E was repeated, this time on the supervised fuzzy maps resulted from FO-SVM. The marking parameters in this case are set to $\Omega_{\min}^C = 20$ and $\Delta\mu_{th} = 0.3$, respectively. All the above approaches are evaluated by means of overall accuracy (OA), average accuracy (AA), kappa coefficient k , and class-specific accuracies. The average OA over the 30 different runs are presented for the two different GeneSIS versions, while the rest accuracies refer to the run exhibiting the maximum OA. GeneSIS was coded in C++, and all experiments were conducted on an Intel Core 2 Quad Q9650 at 3.0 GHz.

The results show that all segmentation-based methods outperform in general the pixel-based SVM, since they combine the SVM evidence with spatial information acquired from segmentation. Only in the trees class, SVM is superior to the comparing methods, indicating thus a drawback of the object-based approaches in handling small sized classes. In regard to the two GeneSIS methods, it can be noticed that both attain similar maximum OA, while the region-based approach performs considerably better than the pixel-based one in terms of average performance. This indicates the enhanced robustness of the proposed scheme in providing, consistently, qualifying results. Moreover, the region-based representation of image data leads to a significant reduction (73%) of execution times. Particularly, pixel-based GeneSIS requires 830.53 (s) while the region-based one needs 222.55 (s), on average. On the other hand, both competing methods are inferior to GeneSIS according to all global accuracy measures. The MSF classifies successfully most of the classes, but fails to handle with the mixed and large classes of meadows and gravel. Contrarily, GeneSIS achieves high accuracies in all classes.

V. CONCLUSIONS

A novel version of the GeneSIS algorithm is presented in this paper, where the main segmentation is performed on an initial region-based map of the image acquired via watershed transform. The effectiveness of the proposed scheme is validated on the classification of a high-resolution hyperspectral image. Comparing to the pixel-based GeneSIS, the execution time is now reduced considerably by an amount of over 70%. At the same time, higher average accuracies are exhibited, indicating enhancement of the method's robustness. Finally, more flexible and arbitrarily shaped objects are obtained, since their shapes are now formed by the boundaries of the watershed objects included in the BSFs.

REFERENCES

- [1] K. S. Fu and J. K. Mui, "A survey on image segmentation", *Pattern Recognition*, vol. 13, pp. 3-16, 1981.
- [2] Y. Tarabalka, J. Chanussot, and J. A. Benediktsson, "Segmentation and classification of hyperspectral images using watershed transformation", *Pattern Recognition*, vol. 43, pp. 2367-2379, 2010.
- [3] D. Li, G. Zhang, Z. Wu, and L. Yi, "An edge embedded marker-based watershed algorithm for high spatial resolution remote sensing image segmentation," *IEEE Trans. Image Process.*, vol. 19, no. 10, pp. 2781-2787, Oct. 2010.
- [4] S. Derivaux, G. Forestier, C. Wemmert, and S. Lefevre, "Supervised image segmentation using watershed transform, fuzzy classification and evolutionary computation," *Pattern Recognit. Lett.*, vol. 31, pp. 2364-2374, 2010.
- [5] S. Makrogiannis, G. Economou, and S. Fotopoulos, "Region dissimilarity relation that combines feature-space and spatial information for color image segmentation," *IEEE Trans. Syst., Man, Cybern. B, Cybern.*, vol. 35, no. 1, pp. 44-53, Feb. 2005.
- [6] S. K. Mylonas, D. G. Stavrakoudis, and J. B. Theoharis, "A GA-based sequential fuzzy segmentation approach for classification of remote sensing images," in *IEEE Int. Conf. Fuzzy Systems*, pp. 1-8, June 2012.
- [7] S. K. Mylonas, D. G. Stavrakoudis, and J. B. Theoharis, "GeneSIS: a GA-based fuzzy segmentation algorithm for remote sensing images," *Knowledge-Based Systems*, vol. 54, pp. 86-102, Dec. 2013.
- [8] A.N. Evans and X.U. Liu, "A morphological gradient approach to color edge detection," *IEEE Trans. Image Process.*, vol. 15, no. 6, pp. 1454-1463, June 2006.
- [9] K. Haris, N. Efstratiadis, N. Maglaveras, and A. K. Katsaggelos, "Hybrid image segmentation using watersheds and fast region merging," *IEEE Trans. Image Process.*, vol. 7, no. 12, pp. 1684-1699, Dec. 1998.
- [10] F. Meyer, "Topographic distance and watershed lines," *Signal Processing*, vol. 38, pp. 113-125, 1994.
- [11] S.-B. Cho and J. H. Kim, "Multiple network fusion using fuzzy logic," *IEEE Trans. Neural Netw.*, vol. 6, no. 2, pp. 497-501, Mar. 1995.
- [12] Y. Tarabalka, J. C. Tilton, J. A. Benediktsson, and J. Chanussot, "A marker-based approach for the automated selection of a single segmentation from a hierarchical set of image segmentations," *IEEE J. Sel. Topics Appl. Earth Observ.*, vol. 5, no. 1, pp. 262-272, Feb. 2012.
- [13] S. P. Moustakidis, G. Mallinis, N. Koutsias, and J. B. Theoharis, "SVM-based fuzzy decision trees for classification of high spatial resolution remote sensing images," *IEEE Trans. Geosci. Remote Sensing*, vol. 50, no. 1, pp. 149-169, Jan. 2012.
- [14] A. Jensen and A. Solberg, "Fast hyperspectral feature reduction using piecewise constant function approximations," *IEEE Geosci. Remote Sens. Lett.*, vol. 4, no. 4, pp. 547-551, Oct. 2007.
- [15] Y. Tarabalka, J. Chanussot, and J. A. Benediktsson, "Segmentation and classification of hyperspectral images using minimum spanning forest grown from automatically selected markers," *IEEE Trans. Syst., Man, Cybern. B, Cybern.*, vol. 40, no. 5, pp. 1267-1279, Oct. 2010.